2011

Transmission Improvement of UMTS and Wi-Fi Signals Through Energy Saving Glass Using FSS

Irfan Ullah
Edith Cowan University

Xiaoli Zhao
Edith Cowan University

Daryoush Habibi
Edith Cowan University

Ghaffer I. Kiani

10.1109/WAMICON.2011.5872858

Transmission Improvement of UMTS and Wi-Fi Signals Through Energy Saving Glass Using FSS

Irfan Ullah, Xiaoli Zhao and Daryoush Habibi
Centre for Communication Engineering Research
Edith Cowan University, WA, Australia
Email: {i.ullah,x.zhao,d.habibi}@ecu.edu.au

Ghaffer Kiani
CSIRO Information and communication technology
Centre, Epping NSW, Australia
Email: ghaffer.kiani@csiro.au

***Abstract*— This paper presents a dual-bandpass (DBP) frequency selective surface (FSS) based on hard-coating energy saving glass (ESG). The objective of this study is to generate a novel design of FSS on ESG, which is to be used for future energy smart buildings at Edith Cowan University (ECU). The ESG is made of a transparent coating of conducting layer on glass substrate, which attenuates infrared (IR) radiations for energy saving purpose. However the coating also attenuates useful UMTS and Wi-Fi signals which are necessary for the communication systems within the University. FSS technique is used to improve transmission of RF/MW signals through ESG by generating an array of patterns in the hard coating layer. The design of the DBP-FSS presented here has achieved transmission requirements for two specific frequency bands, with stable frequency response for both transverse electric (TE) and transverse magnetic (TM) polarization at normal and oblique incidence angles up to 60^0. The double square loop (DSL)-FSS sustains 92.7% efficiency of ESG by attenuating IR radiations. This design methodology can be adapted as a general reference, which is suitable for applications under similar circumstances. Optimized design and theoretical results are presented.**

Keywords- energy saving glass (ESG); bandpass filter (BPF); frequency selective surface (FSS); universal mobile telecommunication system (UMTS), wireless fidelity (Wi-Fi);

I. INTRODUCTION

The use of energy saving glass (ESG) in modern building architecture has become very popular [1] These ESGs are fabricated by applying a uniform thin (0.3-0.4 micron) layer of pyrolytic coating (hard coating) or metal oxide (soft coating) onto the glass substrate, by different processes, for example, chemical vapor deposition (CVD) method. The coating can be deposited on one or both sides of ordinary/float glass [2-4]. The coating layer is able to transmit visible light while reflect infrared radiations (IR) at room temperature [5]. IR insulation is thus achieved, which can be utilized to keep buildings warm in winters and cold in summers, resulting in significant energy savings. As an example, single glazing ESG window is able to increase room temperature by 8 ^{0}C, if outside is at -10 ^{0}C. When a double glazing glass with a thickness of 3-10 mm is used, an increase of 15 ^{0}C can be achieved. Amongst different coating types, hard coating is more durable and easy in handling as compared to soft coating, whereas soft coating provides higher IR attenuation but the metal oxide coating layer can be damaged easily if not handled with care.

However, a related issue associated with the application of ESG is that the coating also attenuates useful RF/microwave signals such as mobile phone, Wi-Fi, security and personal communication signals. Generally speaking the soft coating could result in a 30dB attenuation (suncool ^{TM}) [1] within RF microwave range, while hard coating layers attenuates up to 200 dB within the same frequency band, To overcome this problem, FSS technique can be utilized, which enables transmission of useful RF signals, in addition to the radiations within the visible light wave range, without changing IR attenuation significantly [4].

The FSS is a periodic structure of identical cells in one or two direction. These structures can be categorized into two different types, known as patch type element and aperture type element. The FSS structures have capacitive and inductive properties, which have been scrutinized in previous research works [6, 7]. In principle an FSS is a spatial filter, the transmission of which is a function of angle of incidence, frequency, and polarization of the incident radio frequency (RF) waves. FSSs are frequently used as bandpass, bandstop, lowpass and highpass filters, The concept of which can be explained by considering a periodic array of elements on a planar surface resonating at single or multiple frequencies, where the length of the elements is a multiple of half of the resonant wavelengths ($\lambda_g/2$) [6, 8]. FSSs are widely used for shielding of non-ionized radiations, radomes design and satellite communications [7, 9]. They have also been employed to improve wireless networks [10, 11] and the design of multi-frequency reflector antennas for creating data communication links and scientific research infrastructures [12, 13]. An FSS with multi-band resonance can be achieved in different ways, among which genetic algorithm design, perturbation, and multi element unit cell are basic design methods. The perturbation technique has been implemented to convert single layer, first order band to dual-band [14] and multi-resonant element for obtaining multi-band resonance, i.e. by using concentric rings [15]. Periodic structures of complex unit cell have also been used for designing multi-band FSS [16, 17], such as a substrate having the same geometries with various dimensions [18, 19] or with fragmented geometries [14, 20]. A multi-band FSS with close separation can also be achieved with two closely spaced capacitive loaded ring resonators having the same dimensions, but with different loading capacitance [21]. A narrow band FSS has been achieved in each band because of high performance of each resonator due to capacitive loading. Multi-band resonant elements are generally preferred because they are lighter [22]. The performance of

DSL-FSS [23] has been discussed assuming frequency of first and second band are significantly separate from each others. However, for these patterns angular stability has not received sufficient attention in the literature.

Here we present a DBP-FSS design, using double square loop (DSL) element, which gives stable frequency response at normal and various oblique incidence angles for both TE and TM polarizations.

II. FSS Design Requirement on Campur

This paper discusses a particular design of a DBS-FSS on a hard coated ESG, to be used in future constructions on the Joondalup campus of Edith Cowan University (ECU), Western Australia. The purpose of this design is to improve the transmission of universal mobile telecommunication system (UMTS), 3G mobile and W-LAN signals. These three types of signal are of importance to the day to day communications within the University. Table I presents the frequency bands of UMTS-FDD for Oceania (Australia). Telstra Australia and 3GIS have installed their radio communication base station (RBS) within the university campus, where two major bands are used: for Telstra WCDMA850 f_c = 887 MHz, and for 3GIS WCDMA2100 f_c = 2112 MHz, where f_c is the center frequency of the required passband.

TABLE I. Frequency Allocation of Universal Mobile Telecommunication system (UMTS) – FDD Band for Australia.

Band No	**Frequency-band**	Name	**UL-Frequencies**	**DL-Frequencies**
1	2100	IMT	1920-1980	2110-2170
5	850	CLR	824-849	869-894

In order to improve the transmission of the UMTS-FDD bands through the ERG glass windows, two passbands centered at the aforementioned frequencies need to be implemented. For these frequencies it is necessary to select optimum design, which does not affect the performance of the ESG significantly within the IR range. Although having more options of fine tuning, the aperture or slot type of FSS design is not selected, considering the bandwidth requirement and IR attenuation. The linear relationship between the percentage area removed and percentage increase in visible transmission [4] is the main consideration during the selection of design. To enhance the performance of the ESG and reduce the IR transmission, FSS can also be etched only in some specific parts of glass where RF/MW signal strength is at the maximum level. The higher level is generally found in the nearest buildings to the RBS. This method is also cost effective. The proposed tool for measuring the maximum level of RF/MW signals is a selective radiation meter (SRM)-3006 [24].

III. Simulation Procedure

In this research the frequency domain solver of CST MW Studio 2010 [25], a fully featured electromagnetic analysis and design software, was used for simulating and optimizing the FSS model under study. The full wave simulation technique was used for DBP-FSS, and for various polarization modes and incident angles. To utilize the computational resources effectively, only a single unit cell was designed (see Fig.1), while the performance of the complete structure, including an infinite number of periods along a 2D plane, was evaluated by applying a periodic boundary condition at the four boundaries of the unit cell, which are perpendicular to the FSS plane, and grouped into two pairs, each consisting of two opposite boundaries labeled as source and destination. The incident wave was assumed to be a plane wave, and different transmission modes (TE and TM) at different incident angles were simulated. Due to the fact that the thickness of the coating layers is in an order of magnitude of ~10 micrometers, in our modeling process we use zero thickness as an approximation. The coating is treated as a perfect electric conductor (PEC). Other physical and the geometrical parameters will be discussed in the next section.

IV. FSS Design and Analysis

Different methods have been used for analyzing and optimizing the FSS under study. Beside parametric analysis, some other tuning techniques can also be employed for DSL i.e. optimized algorithms and differential evaluation strategies (DES) [26]. The geometry of our optimized final design of a DBP-FSS unit cell is presented in Fig.1. The cell structure is modeled as two square through-cuts, of different side lengths, on the coating layer. The relative permittivity (ε_r) and conductivity (σ) of glass is 6.9 and 5×10^{-4} S/m, respectively [2].

TABLE II. Parameters of the Dual – Bandpass FSS Unit Cell

Parameters	$P_x \times P_y$	$D_x \times D_y$	$L_x \times L_y$	w_1
Values	40×40 mm	37.5×37.5 mm	20.5 mm	0.5 mm
Parameters	w_2	**g/2**	ε_r	**h**
Values	0.5 mm	0.75 mm	6.9	6 mm

Periodic array is arranged in two dimensions with periodicity of $P_x = P_y$, The distance between the boundary of the unit cell and the larger square is g/2. For the first bandpass filter (for the f_c = 887 MHz band), the length along x - axis and y - axis equal to $D_x = D_y$ and the width is equal to w_2. Whereas for the second bandpass filter (for the f_c = 2112 MHz band), the length along x - axis and y - axis is equal to $L_x = L_y$, and the width is equal to w_1. The values of these parameters are listed in Table II for the center frequencies given above. In this design 7.12% of coating area was removed from the total area of unit cell (see Fig.1). As a result an extra 7.13% IR energy will transmit through the ESG, which represents an insignificant percentage of the total radiations [4].

In our study, other FSS patterns were also simulated for comparison purpose. For example, a combination of square loop and jerusalem cross was tested [27]. However it is observed that DSL gives much higher bandwidth, while jerusalem cross gives less bandwidth but more tuning options with small band of separation [6]. In this research the tuning effect of jerusalem cross was simulated in

parametric analysis using the aperture width as the parameter. The result shows that when the aperture width gradually increases from 0.82 – 0.86 mm, some minor unwanted resonances appear. A gradual increase in the resonant frequency of the stopband occurs during changing in the aperture width, and then random change is observed up to a width of 0.92 mm. The parametric analysis of top loaded element shows that there is a steady gain in bandwidth (with respect to the transmission coefficient of -10 dB) from 774 - 815 MHz with a change in the aperture width from 0.81 - 0.85 mm, after that the bandwidth remains unchanged until 0.91 mm, before finally it starts to create unwanted resonance at oblique incidence angles. The jerusalem cross has matching resonance mode and behaves as a parallel LC equivalent circuit, whereas square loop behaves as a series LC circuit, and gives higher bandwidth without creating extra resonance at oblique incidence angles.

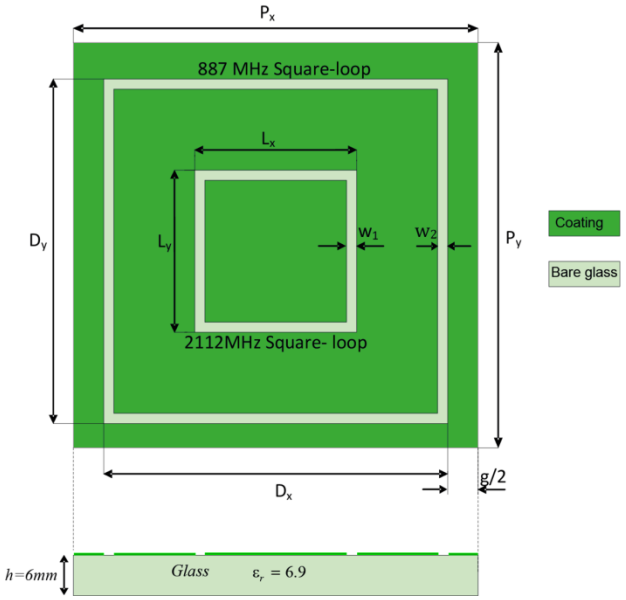

Figure 1. Top – double square dual-bandpass FSS. Bottom – cross sectional view at the center line.

Hence square loop gives better level of transmission within the Wi-Fi signal range without creating unnecessary resonances. The parametric analysis of DSL shows that the resonant frequency of the first passband (outer square loop with a resonance frequency of f_1) does not depend on lengths L_x and L_y of the inner square loop (which has a higher resonant frequency), but it is dependent on the aperture width w_2. On the other hand, the resonant frequency of the inner square loop, having a resonance frequency f_2, is dependent on L_x and L_y, and f_2 increases with the decrease of L_x and L_y. The control of the resonant frequency of the passband (at frequency f_T) depends also on the relative spacing between the first and the second resonance loop.

These observations agree with the results in previous studies, obtained using a different substrate [28].

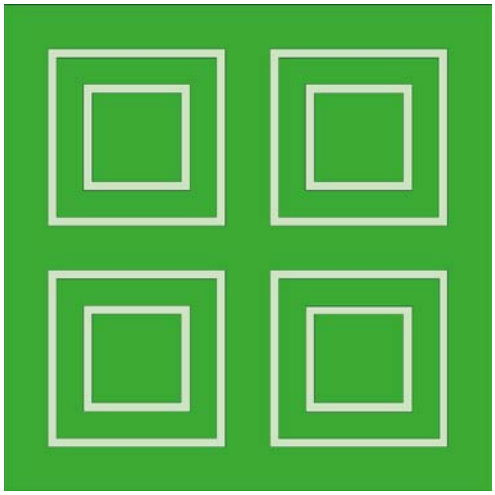

Figure 2. Layout of a portion of FSS in an infinite 2D array, showing 2×2 unit cells.

V. Simulation Results

The simulation results of transmission patterns for the DBP-FSS are presented in Fig. 3 and Fig. 4. Optimization process was carried out step by step using CST MW Studio 2010 for fine tuning. The transmission coefficients for TE and TM polarization were then evaluated and recorded for 0 - 3 GHz frequency at both normal and oblique incidence angles.

A. TE Polarization

In Fig. 3 transmission coefficients (in dB) for TE polarization are given at normal and oblique incidence angles. The resonant frequencies and the corresponding bandwidths are listed in Table III. At all the four resonant frequencies plotted, negligible attenuation is observed. In order to minimize the unwanted absorption within the entire range of the two UMTS bands, the FSS is designed in such a way that, the widths of -10 dB passbands of the filters are significantly wider than those of the corresponding UMTS bands, with the center frequencies slightly tuned to optimize the response. The final design gives a maximum attenuation of only 4 dB over the full WCDMA850 band (824-894 MHz, see Table I), while the -10 dB passband width is between 388 - 651 MHz for different incident angles (Table III). For the full WCDMA2100 band, the maximum attenuation at oblique incidence angle is 7 dB, while the -10 dB passband width ranges between 357 ~ 923 MHz for different incident angles. Note that for a particular mobile station only a smaller range of the full bands is used, as such smaller attenuation can be achieved locally by adjusting the center frequencies. For examples, at ECU site the local band for WCDMA850 is 884.7 – 889.7 MHz, and over this range the maximum attenuation is reduced to 1 dB. Similar reduction is observed for the WCDMA2100 band, with a maximum attenuation of 3 dB. These results satisfy the design requirements to transmit f_c =887 MHz and f_c = 2112 MHz UMTS bands.

As for different incident angles, the first bandstop center frequency is between 1629 ~ 1644 MHz, with attenuation ranging between -62 ~ -73 dB. On the other hand the second

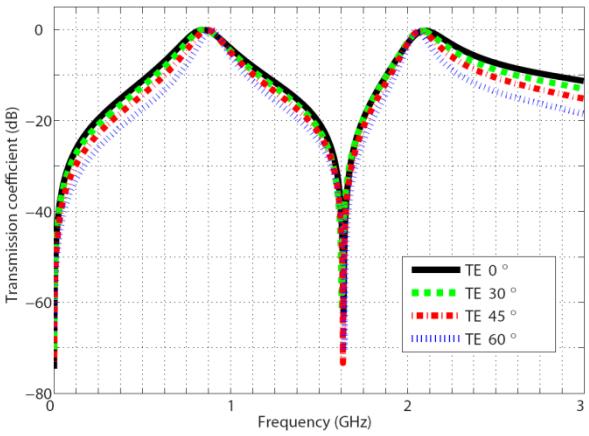

Figure 3. Transmission coefficient of dual-bandpass FSS at normal and oblique incidence angles for TE polarization

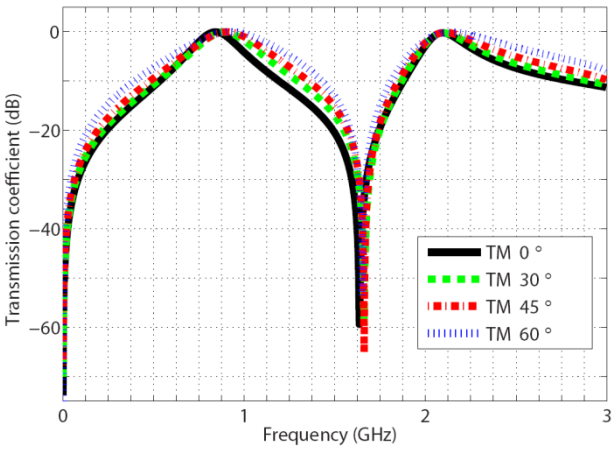

Figure 4.

Figure 5. Transmission coefficient of dual-bandpass FSS at normal and oblique incidence angles for TM polarization

bandstop center frequency is between 3132 ~ 3264 MHz, with attenuation ranging between -40 ~ -54 dB. By using FSS the complete WCDMA850 and WCDMA2100 bands with a TE polarization can be transmitted with less than 6 dB attenuation, for an incident angle $\leq 60^0$. There is only a slight shift of resonance frequency of about 2% in the case of the first passband, and 3% in the case of the second passband, for different incidence angles, which confirms the stability of the FSS at various angles from $0^0 - 60^0$. On the other hand, with the increase of the incident angle from 0^0 to 60^0, there is a significant decrease in the bandwidth for both of the passbands: ~ 40% for the first passband, and ~60% for the second passband. As such, in the case when large incident angles are required, variation of other parameters is necessary in order to achieve desirable performance.

B. TM Polarization

Fig. 4 presents transmission coefficient (dB) for TM polarization at normal and oblique incidence angles. The resonant frequencies and the corresponding bandwidths are listed in Table IV. Again, for all the four resonant frequencies listed, negligible attenuation is observed. Similar discussions with the corresponding TE case are applicable, for the passband resonant frequencies.

On the other hand, compared with the TE polarization, larger bandwidths of the two passbands were observed for the TM polarization. The bandwidth obtained for f_c = 887 MHz band ranges between 655 ~ 1046 MHz, while that for the 2112 MHz band ranges between 921 ~ 1252 MHz, with respect to -10 dB transmission coefficient. There is a decrease in the attenuation at both bandstop centers. Here the first bandstop center frequency is between 1637 ~ 1652 MHz, with attenuation ranging between -47 ~ -63 dB. The second band-stop center frequency is between 3094 ~ 3269 MHz, with attenuation ranging between -34 ~ -47 dB. Again, by using FSS the complete WCDMA850 and WCDMA2100 bands with a TM polarization can be transmitted with less than 6 dB attenuation, for an incident angle $\leq 60^0$. The resonant frequency is also stable over the incident angle range $0^0 - 60^0$.

Furthermore, as discussed above, at a large incident angle (60^0) more than 60% increase in bandwidth can be achieved as compared with 0^0 when using TM polarization. When large bandwidth is required, this factor can be taken into account in the design process.

In summary, the transmission results of both TE and TM polarization satisfy the design requirements given in section II. Under different circumstances the design requirements may be different, which can be achieved using parametric analysis and optimization process.

TABLE III. -10DB TRANSMISSION BANDWIDTH AT 887 MHZ AND 2112 MHZ FOR TE POLARIZATION.

	887 MHz		**2112 MHz**	
Angle	***Resonance (MHz)***	***BW (MHz)***	***Resonance (MHz)***	***BW (MHz)***
TE 0^0	875	651	2112	923
TE 30^0	866	581	2092	730
TE 45^0	885	500	2100	565
TE 60^0	891	388	2076	357

TABLE IV. -10DB TRANSMISSION BANDWIDTH AT 887 MHZ AND 2112 MHZ FOR TM POLARIZATION.

	887 MHz		**2112 MHz**	
Angle	***Resonance (MHz)***	***B.W (MHz)***	***Resonance (MHz)***	***B.W (MHz)***
TM 0^0	861	655	2111	921
TM 30^0	899	766	2105	1032
TM 45^0	909	872	2118	1149
TM 60^0	942	1046	2162	1252

VI. CONCLUSION

In this work design and evaluation of a DBPF-FSS based on hard-coating ESG was carried out, in order to improve the transmission of UMTS bands. The design has been optimized according to the particular requirements to be used at ECU, and the full wave simulation technique has been utilized to evaluate the response of FSS unit cell. The design has achieved transmission requirements for the two specific frequency bands, with stable frequency response for both TE and TM polarization at normal and oblique incidence angles, up to 60^0. The DSL-FSS unit cell design sustains 92.7% efficiency of ESG by attenuating IR radiations, which fulfills the overall design objectives. Details about the effects of parameters have been discussed, with concrete suggestions for variations in the similar design works. This design can be adapted as a general reference, which is suitable for applications under similar circumstances. Experimental works, including fabrication and measurement of the FSS, are under way in our research laboratory to verify the theoretical design and evaluation.

References

[1] Pilkington. *Pilkington group limited*. Available: www.pilkington.com

[2] C. I. Kiani, *et al.*, "Glass Characterization for Designing Frequency Selective Surfaces to Improve Transmission through Energy Saving Glass Windows," in *Microwave Conference, 2007. APMC 2007. Asia-Pacific*, 2007, pp. 1-4.

[3] G. I. KIANI, "Passive, active and absorbing frequency selective surfaces for wireless communication applications," PhD Thesis, Macquaire University, Sydney, 2009.

[4] G. I. Kiani, *et al.*, "Transmission of infrared and visible wavelengths through energy-saving glass due to etching of frequency-selective surfaces," *IET Microwaves, Antennas and Propagation*, vol. 4, pp. 955-961, 2010.

[5] M. Gustafsson, *et al.*, "Design of frequency selective windows for improved indoor outdoor communication," *Antennas and Propagation, IEEE Transactions on*, vol. 54, pp. 1897-1900, 2006.

[6] T. Wu, *Frequency selective surface and grid array*: Wiley-Interscience, 1995.

[7] B. Munk, *Frequency selective surfaces: theory and design*: Wiley-Interscience, 2000.

[8] R. Ulrich, "Far-infrared properties of metallic mesh and its complementary structure," *Infrared Physics*, vol. 7, pp. 37-50, 1967.

[9] W. Kiermeier and E. Biebl, "New dual-band Frequency Selective Surfaces for GSM frequency shielding," in *Microwave Conference, 2007. European*, 2007, pp. 222-225.

[10] G. I. Kiani, *et al.*, "Angle and polarization independent bandstop frequency selective surface for indoor wireless systems," *Microwave and Optical Technology Letters*, vol. 50, pp. 2315-2317, 2008.

[11] G. I. Kiani, *et al.*, "Active frequency selective surface design for WLAN," *10th Australian Symposium on Antennas, Sydney, Australia, 14-15 Feb.* , 2007.

[12] G. Schennum, "Frequency-selective surfaces for multiple-frequency antennas Design data plus experimental results," *Microwave Journal*, vol. 16, pp. 55-57, 1973.

[13] V. Agrawal and W. Imbriale, "Design of a dichroic Cassegrain subreflector," *Antennas and Propagation, IEEE Transactions on*, vol. 27, pp. 466-473, 2002.

[14] R. A. Hill and B. A. Munk, "The effect of perturbating a frequency-selective surface and its relation to the design of a dual-band surface," *Antennas and Propagation, IEEE Transactions on*, vol. 44, pp. 368-374, 1996.

[15] J. Romeu and Y. Rahmat-Samii, "Fractal FSS: a novel dual-band frequency selective surface," *IEEE Transactions on Antennas and Propagation*, vol. 48, pp. 1097-1105, 2000.

[16] W. Te-Kao and L. Shung-Wu, "Multiband frequency selective surface with multiring patch elements," *Antennas and Propagation, IEEE Transactions on*, vol. 42, pp. 1484-1490, 1994.

[17] W. Te-Kao, "Four-band frequency selective surface with double-square-loop patch elements," *Antennas and Propagation, IEEE Transactions on*, vol. 42, pp. 1659-1663, 1994.

[18] J. P. Gianvittorio, *et al.*, "Self-similar prefractal frequency selective surfaces for multiband and dual-polarized applications," *Antennas and Propagation, IEEE Transactions on*, vol. 51, pp. 3088-3096, 2003.

[19] Y. Junho and R. Mittra, "Numerically efficient analysis of microstrip antennas using the Characteristic Basis Function method (CBFM)," in *Antennas and Propagation Society International Symposium, 2003. IEEE*, 2003, pp. 85-88 vol.4.

[20] D. H. Werner and D. Lee, "A design approach for dual-polarized multiband frequency selective surfaces using fractal elements," in *Antennas and Propagation Society International Symposium, 2000. IEEE*, 2000, pp. 1692-1695 vol.3.

[21] X. Rong-rong, *et al.*, "Dual-Band Capacitive Loaded Frequency Selective Surfaces With Close Band Spacing," *Microwave and Wireless Components Letters, IEEE*, vol. 18, pp. 782-784, 2008.

[22] M. Salehi and N. Behdad, "A Second-Order Dual X-/Ka-Band Frequency Selective Surface," *Microwave and Wireless Components Letters, IEEE*, vol. 18, pp. 785-787, 2008.

[23] R. U. Nair, *et al.*, "EM performance analysis of double square loop FSS embedded C-sandwich radome," in *Applied Electromagnetics Conference (AEMC), 2009*, 2009, pp. 1-3.

[24] NARDA. (2009, *Selective Radiation Meter 3006 (2010 ed.)*. Available: www.narda-sts.de

[25] CTS. *CST Microwave studio (2010 ed.)*. Available: www.cst.de

[26] X. F. Luo, *et al.*, "Design of double-square-loop frequency-selective surfaces using differential evolution strategy coupled with equivalent-circuit model," *Microwave and Optical Technology Letters*, vol. 44, pp. 159-162, 2005.

[27] I. ULLAH, *et al.*, "Transmission improvement of mobile phone signals through energy saving glass using frequency selective surface," *12th Australian symposium on Antenna, Sydney*, 2011.

[28] R. J. Langley and E. A. Parker, "Double-square frequency-selective surfaces and their equivalent circuit," *Electronics Letters*, vol. 19, pp. 675-677, 1983.